Energy, Environmental, and Catalysis Applications

A Highly-Efficient and Stable Catalyst based on Co(OH)2@Ni Electroplated on Cu-Metallized Cotton Textile for Water Splitting

Zining Wang, Shan Ji, Fusheng Liu, Hui Wang, Xuyun Wang, Qizhao Wang, B Pollet, and Rongfang Wang

ACS Appl. Mater. Interfaces, **Just Accepted Manuscript** • DOI: 10.1021/acsami.9b07371 • Publication Date (Web): 25 Jul 2019

A Highly-Efficient and Stable Catalyst based on $Co(OH)_2$@Ni Electroplated on Cu-Metallized Cotton Textile for Water Splitting

Zining Wang [†], Shan Ji[†,‡], Fusheng Liu[†], Hui Wang[†]**, Xuyun Wang[†], Qizhao Wang[§], Bruno G. Pollet[⁄⁄], Rongfang Wang[†]****

[†] State Key Laboratory Base for Eco-Chemical Engineering, College of Chemical Engineering, Qingdao University of Science and Technology, Qingdao, 266042, China

[‡] College of Biological, Chemical Science and Chemical Engineering, Jiaxing University, Jiaxing, 314001, China

[§] College of Chemistry and Chemical Engineering, Northwest Normal University, Lanzhou, 730070, China

[⁄⁄] Department of Energy and Process Engineering, Faculty of Engineering, Norwegian University of Science and Technology (NTNU), NO-7491 Trondheim, Norway

KEYWORDS: α-$Co(OH)_2$; Hydrogen Evolution Reaction; Oxygen Evolution Reaction; Bifunctional Catalyst; Water Electrolysis.

ABSTRACT: The concept of using renewable energy to power water electrolyzers is seen as a favorable approach for the production of green and sustainable hydrogen. The electrochemical water splitting can be significantly and efficiently enhanced by using bifunctional catalysts, active towards both the OER (oxygen evolution reaction) and the HER (hydrogen evolution reaction). Herein, a stable and highly performing catalyst based upon hybrid metal/metal hydroxide nanosheet arrays electroplated onto Cu-metallized cotton textile ($Co(OH)_2$@Ni) was designed and fabricated as a bifunctional electrocatalyst for the complete water splitting reactions. It was found that the interconnected α-$Co(OH)_2$ nanosheets were evenly formed onto the metalized cotton textile, and the optimized $Co(OH)_2$@Ni sample exhibited an overpotential of +96 mV at 10 mA cm^{-2}, with excellent stability towards the HER. The *as*-prepared catalyst also showed superior electrochemical activity and durability towards the OER, which was found to be comparable to conventional precious group metal (PGM)-based catalysts. In addition, when $Co(OH)_2$@Ni were assembled as the electrodes in a water electrolyzer (1 M KOH), a cell voltage of 1.640 V was achieved at a current density of 10 mA cm^{-2}, enabling it to be a promising bifunctional catalyst for water electrolysis in real applications.

1. INTRODUCTION

Hydrogen from water electrolyzers is now seen as an encouraging energy carrier for stationary and mobile applications; and when used in a fuel cell, it only produces water.[1-4] Thus, it is a renewable and practically infinite resource. During water electrolysis, the key processes are a series of electrocatalytic reactions, namely the OER (oxygen evolution reaction) occurring at the anode and the HER (hydrogen evolution reaction) occurring on the cathode.[5-7] However, expensive precious group metal (PGM) catalysts are usually used as catalyst materials for the HER and OER due to their low anodic and cathodic overpotentials ($\eta_{a,c}$), which seriously hinders

the practical application of water electrolysis.[8-9] Over the last decade, the strategy for replacing PGM catalysts by non-precious metal ones (NMPC) materials has been a dynamic research topic in the area of hydrogen and fuel cells.[10-11]

Transitional-metal-based catalysts, for example, sulphides,[12-13] hydroxides,[14-15] selenides,[16-17] have been intensively investigated as encouraging substitutes to noble metal OER and HER electrocatalysts. It has been shown that the development of binary transitional metal-based materials, such as metal/alloy materials and metal oxides/hydroxides, could further improve the electrochemical performance for water splitting due to the synergistic effect.[18-19] For example, it has been recently demonstrated that $Ni(OH)_2/Ni_3S_2$ nanosheets exhibited remarkable improved OER and HER activities of low overpotentials i.e. +270 mV and +211 mV at a current density of 20 mA cm^{-2}, respectively.[15] Although great advances have been made in the generation of transitional metal-based catalyst materials, their performance is still not comparable to that of PGM catalysts.

To greatly enhance the electrochemical properties of transitional metal-based catalysts, the microstructure of the catalysts could be re-engineered and tuned, since it has a significant impact on the mass and charge transfer during the electrocatalytic processes.[10, 20-21] At present, the electrode material of integrated architecture, i.e. in which the active component with an array characteristic is uniformly distributed on a three-dimensionally porous current collector without binder, is thought to be a promising catalyst for water electrolysis.[2, 22-23] In such a structure, the interface/chemical distribution is homogeneous at the nanoscale and a fast ion and electron transfer is guaranteed. For example, $CoNiSe_2$ hetero-nanorods decorated with LDH (layered double hydroxide) nanosheets are produced on nickel foam to form a bind-free three-dimensional electrode; in this configuration the selenide-LDHs interfaces may be able to enhance the

chemisorption of water to generate reactive H intermediate, yielding in rapid hydrogen evolution reaction kinetics.[24] So far, most of the works in the area of water electrolysis are related to these materials using nickel foam and carbon materials as conductive matrices. The hydrophobicity of these two materials is detrimental to the electrocatalytic process. Cotton fibers are highly hydrophilic and can absorb a large amount of water or other polar solvents .[25] By coating a conductive layer on its surface, cotton textile could be used as current collector .[26] Thus, the electrode materials of integrated structures deposited on conductive cotton textile might result in high electrocatalytic performance for water electrolysis.

In this study, an approach for producing a novel hybrid metal/metal hydroxide nanosheet arrays on Cu-metallized cotton textile was developed as dual-functional electrocatalyst for the generation of oxygen and hydrogen. This unique structure has the following advantages: firstly, it includes nickel (Ni), which endows the catalyst with good conductivity, and $Co(OH)_2$ can chemisorb the H_2O molecular and facilitate the catalytic process; secondly, the open structure of $Co(OH)_2$ nanosheets can make the underlying Ni layer accessible to the electrolyte and the Ni layer is directly in contact with the current collector to ensure fast electron transfer; thirdly, cotton has hierarchical structures possessing high surface areas, large porosity, and hydrophilic functional groups. Such specific structures can boost the specific surfaces of the active materials and allow the electrodes to be well-wetted by an aqueous electrolyte. The results show that the optimized sample (Ni-Co-30) developed in this investigation exhibited high HER electrochemical reactivity. For example, the overpotential and Tafel slope values for the hydrogen evolution reaction were found to be +96 mV (at a current density of 10 mA cm^{-2}) and 104.2 mV dec^{-1} respectively. The sample (Ni-Co-30) also showed higher OER performance i.e. the overpotential and Tafel slope values were found to be +300 mV (at

10 mA cm^{-2}) and 70.1 mV dec^{-1} respectively. Moreover, it is further demonstrated that the Ni-Co-30 employed as cathode and anode in H_2O electrolysis can deliver 10 mA cm^{-2} at 1.640 V with greatly improved stability.

2. EXPERIMENTAL METHODS

2.1 Material Synthesis

In this study, all analytical grade (AR) chemicals were employed without any further purification. Before sputtering copper (Cu) on the surface of the textile substrate, a piece of cotton cloth with a size of 10 × 10 cm^2 (thickness: 0.36 mm) was ultrasonically clean in ethanol and ultrapure water sequentially, and then dried at 60 ^oC in a vacuum oven. After that, both sides of the cotton cloth sample were sputtered with Cu using 99.99% of pure copper as a target, which was labeled as "Cu". Subsequently, the nickel (Ni) layer was electroplated onto the obtained cloth in a two-electrode electrochemical cell. In this cell, a pure Ni metal and a Cu sputtered cloth was used as the positive and the negative electrodes respectively. A solution containing $NiSO_4$ (300 g/L), $NiCl_2$ (45 g/L), H_3BO_3 (35 g/L) and sodium dodecyl sulfate (SDS, 0.05 g/L) was used to electroplate Ni onto the cloth. During the electroplating step, a constant current of 10 mA cm^{-2} was applied to the electrochemical cell for 30 min. After that, the obtained cloth was rinsed in pure water and ethanol alternatively, and then dried at 60 ^oC in a vacuum oven. The obtained cloth was labeled as "Ni-Cu".

Before $Co(OH)_2$ was electrodeposited onto the surface of Ni-Cu, the Ni-Cu was washed with pure ethanol and ultrapure water. The electrolyte used for electrodeposition was 0.05 M $Co(NO_3)_2$. The electrodeposition experiments were performed out in a 3-electrode electrochemical cell by cyclic voltammetry for 30 cycles over a potential range of -1.2 to -0.8 V *vs.* Ag/AgCl at a scan rate of 50 mV s^{-1}. In this electrochemical cell, the cleaned "Ni-Cu" sample

was employed as the WE (working electrode), Pt as CE (counter electrode) and Ag/AgCl as RE (reference electrode). After electrodeposition, the obtained electrode was washed with pure water and then dried in a vacuum oven for 12 hours. The *as*-prepared electrode was labeled as "Ni-Co-X" (X: CV cycling number).

2.2 Physical Characterization

XRD (X-ray diffraction) spectra of the *as*-prepared catalysts were generated on a Shimadzu XD-3A (Japan), using filtered Cu-Kα radiation (λ = 0.15418 nm), generated at 40 kV and 30 mA. Scans for 2θ values were recorded at 5° min^{-1} between 10° and 80°. SEM (scanning electron microscopy) images were obtained using a Carl Zeiss Ultra Plus electron microscope. Scans for 2θ values were recorded at 4° min^{-1} between 10° and 80°. TEM (Transmission electron microscopy) images were taken on a JEOL (JEM-2000 FX) microscope operating at 200 kV. XPS (X-ray photoelectron) spectra were generated using a VG Escalab210 spectrometer fitted with Mg 300 W X-ray source.

2.3 Electrochemical Characterization

The HER and OER electrochemical performances were evaluated in a 3-electrode electrochemical cell connected to a potentiostat/galvanostat (CHI 660, CH Instruments, Inc., Shanghai). During the testing, the reference electrode (RE) and counter electrode (CE) was a Hg/HgO and a graphite rod respectively. LSV (linear sweep voltammetry) and CV (cyclic voltammetry) voltammograms were performed in a 1.0 M potassium hydroxide (KOH) electrolyte. EIS (Electrochemical impedance spectroscopy) spectra were measured at corresponding OER and HER electrode potentials from 0.01 to 1,000,000 Hz with an amplitude of 5 mV. To evaluate the "Ni-Co-X" performance in the overall water splitting, "Ni-Co-X"

was used as cathode and anode in a 2-electrode cell configuration. LSV voltammograms were recorded at a scan rate of 5 mV s^{-1}. All potentials stated in this study, are referenced to a RHE (reversible hydrogen electrode). *iR* compensation (90%) was used for all electrochemical experiments.

3. RESULTS AND DISCUSSION

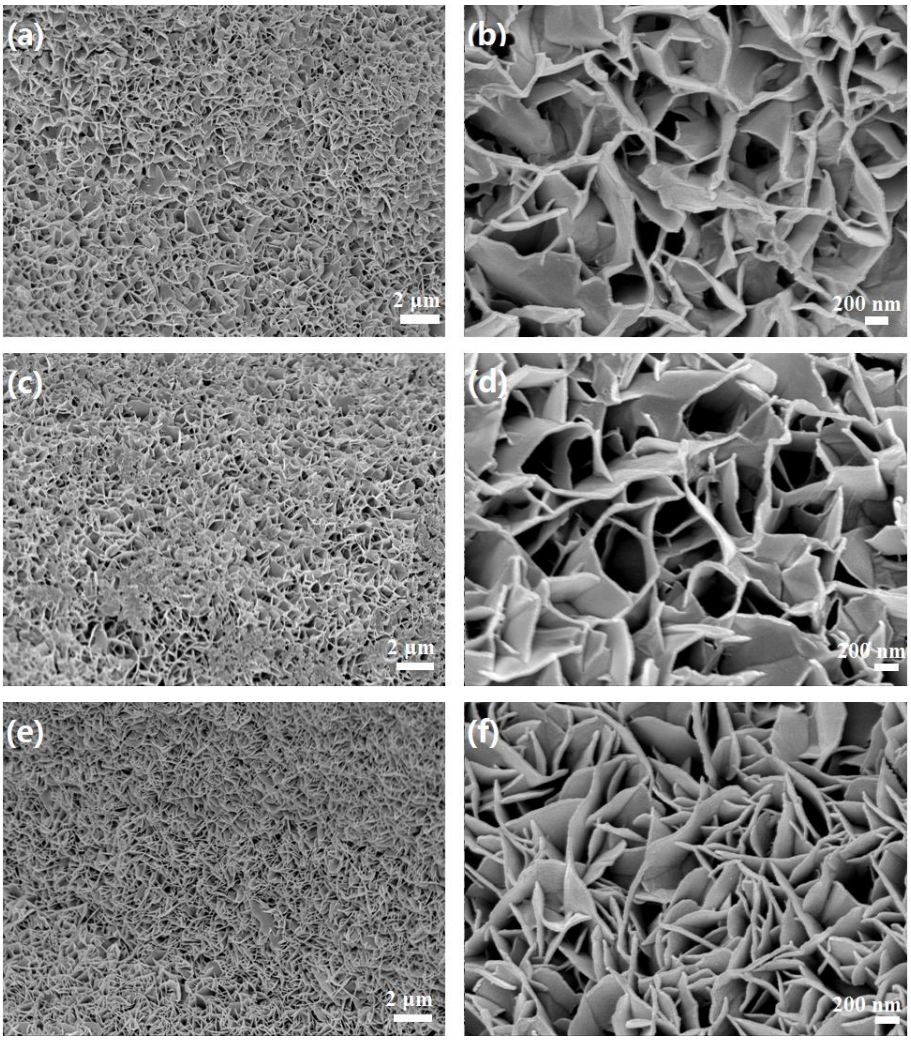

Figure 1. SEM pictures of Ni-Co-Cu electrodes synthesized under various CV cycles (a,b) Ni-Co-20; (c,d) Ni-Co-30; (e,f) Ni-Co-40.

In this study, a novel cotton-based material was developed to support $Co(OH)_2$ nanosheets as water splitting electrocatalyst material having dual functionality. Firstly, cotton was sputtered with copper (Cu) onto its surface to make cotton electrically conductive. After that, the cotton-Cu sample was electrochemically coated with nickel (Ni) on its surface to improve the electrical conductivity and electrochemical stability. Subsequently, the $Co(OH)_2$ layer was electrodeposited on the surface of Ni-Co via cyclic voltammetry. Figure S1 shows the color of the blank cotton textile, Cu-metalized cotton, Ni-coated cotton, and $Co(OH)_2$@Ni. The morphology of the "Ni-Co-X" samples synthesized via cyclic voltammetry was evaluated by scanning electron microscopy (SEM). As represented in Figure 1(a, c and e), interconnected $Co(OH)_2$ nanosheets were evenly formed onto the surface of "Ni-Cu". There is no obvious change of the sheet-like morphology when electrochemical deposition occurred in the range of 20 to 40 CV cycles. As presented in the zoomed SEM images in Figure 1(b, d, and f), the $Co(OH)_2$ nanosheets became denser with an increased number of CV cycles. These figures also show that $Co(OH)_2$ nanosheets of the three samples were interconnected with each other, forming a three-dimensional configuration with an open structure. In such a structure, the more exposed surface is in contact with the electrolyte, which can in turn efficiently facilitates the ion and electron transfer during the electrochemical processes.[29-30]

The crystal phase of the *as*-prepared Ni-Co-30 was investigated by XRD. As presented in Figure 2(a), characteristic diffusion peaks of Ni at 44.6°, 51.8° and 76.6° corresponding to the (111), (200), and (220) planes of the face-centered cubic Ni (JCPDS No.70-0809) and Cu at 43.34°, 50.46° and 74.18° related to the (111), (200), and (220) planes of the face-centered cubic Cu (JCPDS No.70-3039), were observed in the XRD pattern of Ni-Co-30. These characteristic peaks of α-$Co(OH)_2$ according to the JCPDS No.46-0605 are clearly shown in the XRD pattern

over the range of 10 - 60°. The intensities of the peaks of $Co(OH)_2$, compared to those of Ni and Cu, are low, indicating that the $Co(OH)_2$ nanosheets with low crystallinity were formed onto the Ni-Co-30. α-$Co(OH)_2$ possesses a hydrotalcite-like structure containing positively charged $Co(OH)_{2-x}(OH)_x$ layers as well as balancing anions accumulated between the hydroxide layers. Due to its larger interlayer spacing, this type of material has been shown to be better than β-$Co(OH)_2$ in terms of electrochemical activities.[31] In addition, the peak of (003) plane is much higher than the others, implying that the $Co(OH)_2$ crystal is preferred to form along the (003) plane direction with larger interlayer space than the other planes. These larger interlayer spaces are able to accumulate more electrolyte ion and improve the contact between the electrolyte and the electrode.

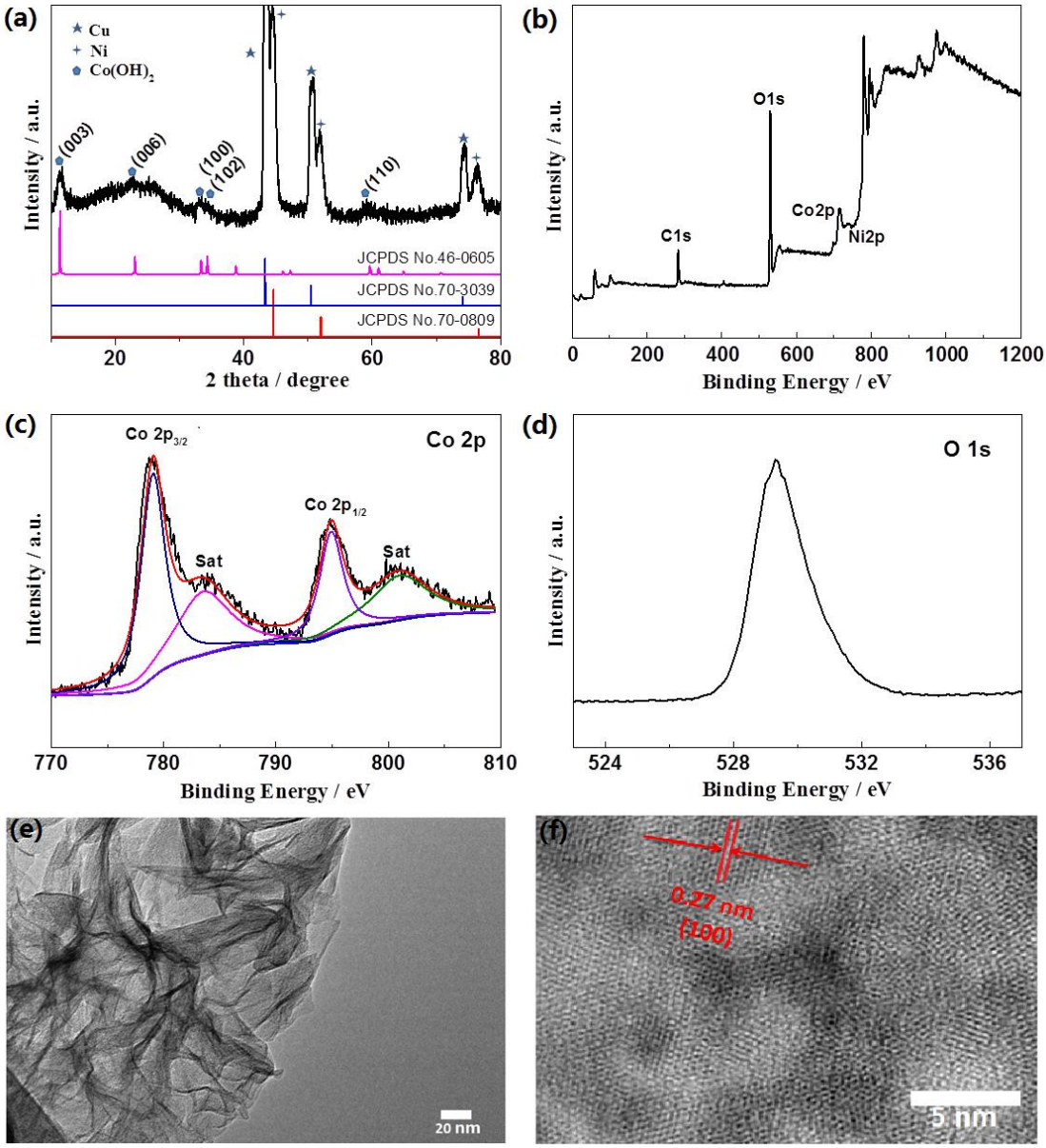

Figure 2. (a) XRD pattern of Ni-Co-30; (b) Survey XPS spectrum of Ni-Co-30; (c,d) The deconvoluted HR XPS spectra of Co *2p* (c) and O *1s*; (d) for Ni-Co-30 electrode; (e) TEM image and (f) HR TEM image of Ni-Co-30.

XPS analyses were performed to probe the Ni-Co-30 chemical state and surface composition as presented in Figure 2(b-d). Figure 2(b) shows the presence of C *1s*, Ni *2p*, O *1s* and Co *2p* in the Ni-Co-30. The signal for Cu was not observed since the XPS can only detect the elements

which are close to the surface (within a range of 4 nm), [32] indicating that the Cu layer was fully covered with Ni and $Co(OH)_2$. Figure 2(b) also shows that the intensity of Co peak is much higher than that of Ni, indicating that Ni layer was further covered by $Co(OH)_2$. The XPS signal of Co *2p* may be fitted into 4 peaks at 783.5 eV, 801.0 eV, 779.1 eV, and 794.9 eV, corresponding to two spin-orbit doublet, i.e. Co $2p_{3/2}$ and Co $2p_{1/2}$, as well as 2 shake-up satellites, indicating the existence of Co with oxidation state in Ni-Co.[33-34] The binding energy at 869.9 eV indicates that only Co oxide existed on the surface of Ni-Co-30.[35]

TEM analyses were further performed to study the morphology of the Ni-Co-30. The TEM image (Figure 2(e)) shows that $Co(OH)_2$ nanosheets possess rough surfaces, on which many wrinkles and grain boundaries may be seen. Figure 2(f) shows a HR TEM image, and well-defined lattice fringes with a *d*-spacing distance of 0.27 nm corresponding to (100) crystalline plane of α-$Co(OH)_2$ can be observed, further confirming that α-$Co(OH)_2$ covered the surface of the Ni-Co-30.

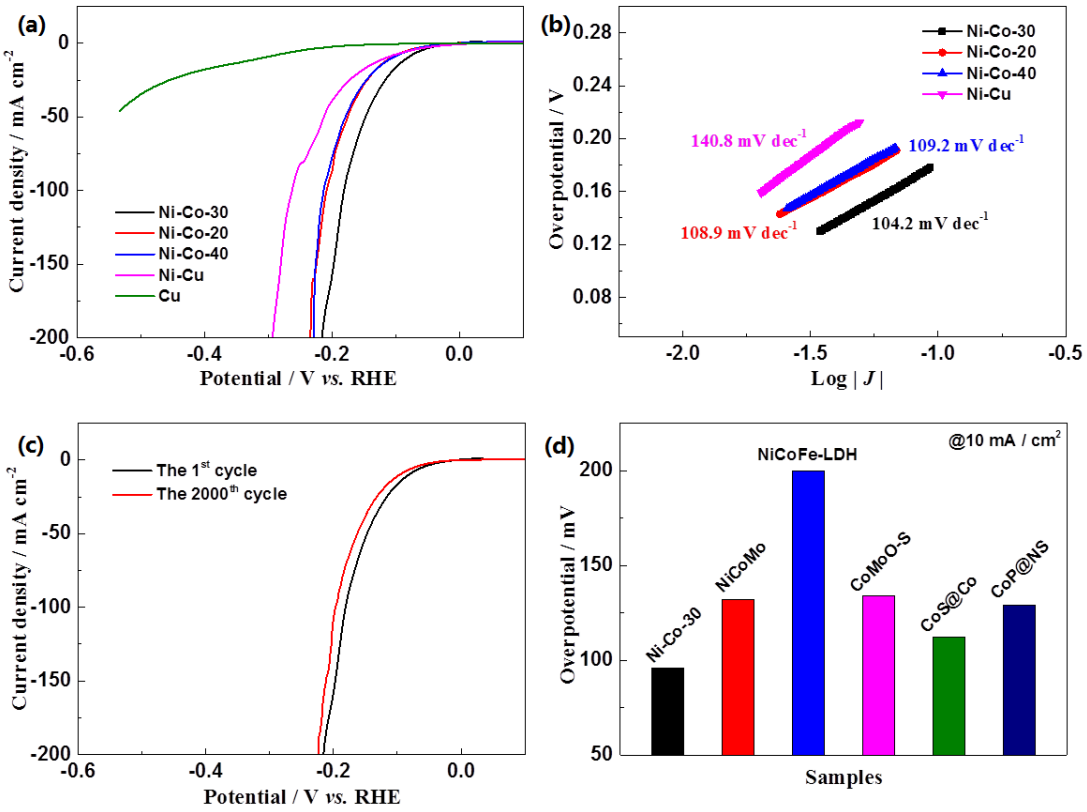

Figure 3. HER electrocatalytic measurements in 1.0 M KOH. (a) LSV voltammogram; (b) Tafel plots; (c) HER LSV curves for the 1st and 2,000th cycles; (d) Overpotentials comparison for all samples at j = 10 mA cm^{-2}.

The hydrogen evolution reaction electrocatalytic activity of "Ni-Cu" and "Ni-Co-X" synthesized with various CV cycles were evaluated in 1.0 M potassium hydroxide (KOH). As presented in Figure 3(a), the Cu sample exhibits poor activity towards the HER. After Ni was deposited, the Ni-Cu became active towards the HER, indicating that Ni layer is active for HER. The onset potentials of Ni-Cu, Ni-Co-20, Ni-Co-30, Ni-Co-40 were -140 mV, -122 mV, -96 mV and -124 mV (*vs.* RHE) respectively. The onset potentials of all Ni-Co samples were more negative than that of the Cu-Ni sample, implying that the $Co(OH)_2$ layer had a crucial role in enhancing the HER activity. For the Ni-Co-30 sample, a HER overpotential was found to be +96

mV (at 10 mA cm^{-2}), a value which was lower than all the other samples, in other words, Ni-Co-30 exhibited the highest HER activity among all tested samples. The overpotentials of all "Ni-Co-X" samples were lower than +150 mV, making them useable for practical water splitting applications. To further shed light on the HER process occurring on these electrodes, Tafel plots were generated (Figure 3(b)) from the polarization curves shown in Figure 3(a). Three steps are involved in the HER process, namely *Volmer*, *Heyrovsky* and *Tafel* steps.[36] In our conditions, the hydrogen evolution reaction occurring on the "Ni-Co-X" electrodes went through the *Volmer-Heyrovsky* step, in which the HER *rds* (rate determining step) is the electrochemical desorption. The HER overpotential (at 10 mA cm^{-2}) for the Ni-Co-30 sample was also compared with some representative Co-based electrocatalysts previously reported in other studies (shown in Table S1 and Figure 3(d)), which clearly highlights that Ni-Co-30 is one of the best catalysts among them in terms of low overpotential (i.e. +96 mV).

Durability is another critical parameter when developing and evaluating electrocatalysts for water splitting. The durability experiments were conducted by CV for 2,000 cycles in 1.0 M KOH electrolyte. The 1^{st} and the $2{,}000^{th}$ cycles LSV curves of Ni-Co-30 and "best" and commercial hydrogen evolution reaction catalyst, Pt/C, are presented in Figure 3(c) and Figure S2(a). After the durability experiments, the overpotential of Ni-Co-30 shifted by +12 mV, which was lower than the overpotential shift of + 32 mV for Pt/C.

Although the SEM results show that the three "Ni-Co-X" samples have similar morphologies, the $Co(OH)_2$ nanosheet densities are slightly different, which could result in different effective surface areas formed on the "Ni-Co-X". To assess the effective surface area, the CV method was employed to quantity the electrochemical double-layer capacitance for these "Ni-Co-X" samples based upon reported methods.[6] A potential window from 0.46 to 0.56 V for the CV experiment

was carefully chosen to avoid any involvement of *Faradaic* currents. Their corresponding CV voltammograms at various scan rates are presented in Figure S3. The obtained corresponding capacitance values are presented in Figure S4(a), indicating that the Ni-Co-30 sample has the highest capacitance among all four samples, namely the CV cycle number for depositing $Co(OH)_2$ has a significant impact on the effective surface area. Moreover, it appears that there is an optimized CV cycle number for growing $Co(OH)_2$ nanosheets onto the Ni layer surface. For example, when the CV cycle number is low, not enough $Co(OH)_2$ nanosheets are formed onto the Ni layer. However, when the CV cycle number is too high, the $Co(OH)_2$ nanosheets formed on the Ni layer could be too dense, in turns making some nanosheets inaccessible for the electrolyte during the electrochemical processes. The electrode kinetics were further studied by EIS (electrochemical impedance spectroscopy) under these conditions. *Nyquist* plots at high-frequency ranges were found to be of semi-circles (Figure S4b), relating to the charge-transfer resistance (R_{ct}). The R_{ct} of Ni-Co-30 was found to be the lowest among all the samples. The EIS result revealed that the $Co(OH)_2$ nanosheets formed after 30 CV cycles could bring more exposed surface area in contact with the electrolyte, resulting in a better charge-transfer during the HER. In this investigation, the authors used the same technique to electrodeposit on the surface of Ni foam (NF) and Carbon fiber cloth (CF). The performance of the Ni-Co-30 sample was obviously better than that of CF-30 and NF-30 (Figure S4c).

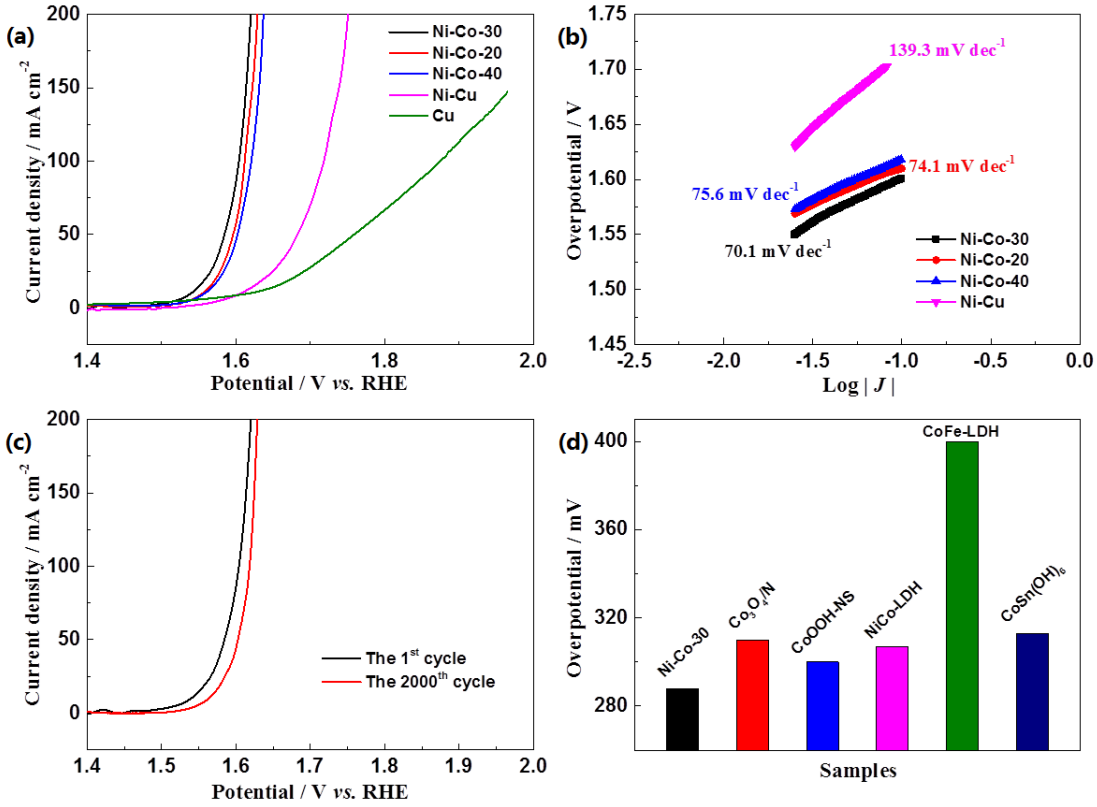

Figure 4. OER electrocatalytic measurements in 1.0 M KOH. (a) LSV curves; (b) Tafel plots; (c) OER LSV curves for the 1st and the 2,000th cycles; (d) Overpotentials comparison at j = 10 mA cm^{-2} for all samples.

The OER activity for Ni and "Ni-Co-X" samples was further investigated in a 1.0 M KOH electrolyte by LSV (scan rate of 5 mV s^{-1}). The obtained LSV voltammograms are presented in Figure 4(a). It may be observed from the figure that the Cu sample exhibits poor activity towards OER, and a relatively good OER activity can be achieved after Ni was deposited. The three "Ni-Co-X" samples are more active towards the OER than Cu and Cu-Ni, especially the Ni-Co-30 sample. The OER onset potential for the Ni-Co-30 sample was similar to that of the "best" OER RuO_2 catalyst reported by Wang *et al.* ,[9] in other words, the OER activity of Ni-Co-30 is comparable to that of RuO_2. Tafel plots were also produced to evaluate the samples OER kinetics. Their corresponding Tafel slopes are shown in Figure 4(b), showing that the Ni-Co-30

catalyst has the lowest Tafel slope, indicating that Ni-Co-30 has a better OER kinetics than the other three materials. Since the rapid charge-transfer kinetics usually results in high OER electrocatalytic performance, EIS (electrochemical impedance spectroscopy) was performed on these electrodes under OER operating conditions. *Nyquist* plot at high-frequency range indicates that electrode kinetics charge-transfer resistance. As shown in Figure S5, Ni-Co-30 exhibited the lowest resistance in the OER, implying that the charge-transfer on Ni-Co-30 was better than the other three samples.

Durability experiments of Ni-Co-30 and RuO_2 catalysts were conducted by continuous OER CV for 2,000 cycles in 1.0 M KOH. The Ni-Co-30 catalyst OER onset potential changed from +1.530 to +1.551 V vs. RHE, i.e. slightly increased by +21 mV after durability testing. This shift of onset potential for the RuO_2 catalyst was found to be +45 mV after the 2,000th LSV cycle (Figure S2(b)). The OER durability testing showed that the Ni-Co-30 catalyst had an excellent stability towards the OER in an alkaline electrolyte. The OER overpotential (at 10 mA cm^{-2}) for the Ni-Co-30 catalyst was benchmarked against those of several other Co-based OER catalysts as shown in Figure 4(d) and Table S2, indicating that the Ni-Co-30 catalyst is a very hopeful OER non-noble metal electrocatalysts among other OER catalysts previously reported in the literature.

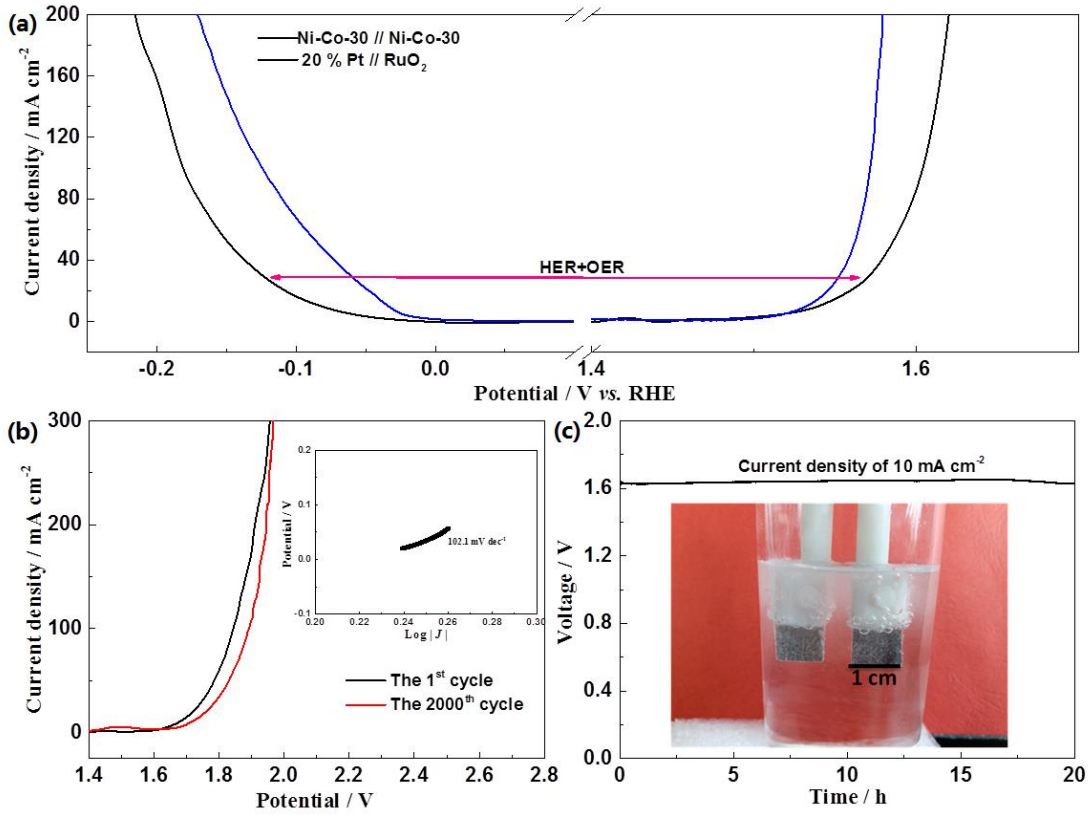

Figure 5. Electrocatalytic measurements for overall water splitting in 1.0 M KOH. (a) Linear sweep voltammogram for HER and OER; (b) Polarization curves of the hierarchical $Co(OH)_2$ nanosheets for overall water splitting and Tafel plots Tafel plots for Ni-Co-30; (c) Chronopotentiometry analyses in a 2-electrode set up at a constant current density (10 mA cm^{-2}) were performed and a picture of the overall water splitting cell.

To evaluate the performance of the hydrogen and oxygen evolution reactions of the Ni-Co-30 catalyst in "real" water electrolysis conditions, the Ni-Co-30 catalyst was used as both the anode and the cathode in 1 M KOH in a two-electrode cell (Ni-Co-30||Ni-Co-30 electrolyzer). The hydrogen and oxygen evolution reaction polarization curves are shown in Figure 5(a). A cell voltage of 1.640 V was achieved at 10 mA cm^{-2}. Although the cell voltage was still higher than that observed for Pt/C||RuO_2 (Ni foam) (1.558 V), Table S3 shows that our reported cell voltage is much lower than many others reported Co-based water electrolyzers. The durability of the Ni-

Co catalyst for the overall water splitting was further evaluated by 2,000 continuous cycles. The corresponding LSVs for the 1st and 2,000th cycles are shown in Figure5(b). After cycling, the cell voltage increased by +15 mV (i.e. from 1.640 V to 1.655 V). For comparison purposes, durability experiments were also performed on the Pt/C||RuO_2 (Ni foam) cell. The cell voltage for Pt/C||RuO_2 (Ni foam) increased by +36 mV (Figure S2(c)), a value which is much higher than that of Ni-Co-30||Ni-Co-30 cell; therefore in our conditions, the Ni-Co-30 catalyst showed better durability than RuO_2 and Pt/C for the complete water splitting electrochemical reactions. Moreover, in the durability study (Figure 5(c)) carried out by continuous electrolysis at a constant current density (10 mA cm^{-2}), a cell voltage of ca. 1.640 V was stable for over 20 hours of operation with negligible degradation. The Ni-Co-30 catalyst morphology was also retained as shown in Figure S6. A picture of the Ni-Co-30||Ni-Co-30 electrolyzer cell is shown in Figure 5(c), in which H_2 and O_2 gas bubbles were generated on both electrodes, further indicating the highly electrocatalytic activity of the Ni-Co-30 catalyst.

4. CONCLUSIONS

A novel structured $Co(OH)_2$ nanosheet material was successfully electrodeposited onto a Ni-coated metalized cotton textile to form a hybrid of metal/metal hydroxide electrocatalyst for the HER and the OER. The Ni-Co-30 exhibited high HER and OER electrocatalytic activities with excellent durability, which in some cases, outclassed most of the Co-based HER and OER catalysts reported other investigations. Its oxygen evolution performance was comparable to that of the "best" RuO_2 catalyst. Moreover, the Ni-Co-30 electrodes were assembled as cathode and anode in a "real" water electrolyzer in the presence of 1.0 M KOH. The assembled electrolyzer produced a cell voltage of 1.640 V at a current density of 10 mA cm^{-2}. The Ni-Co-30 electrodes exhibited better durability than that of the Pt/C||RuO_2 used for water electrolysis. This

investigation highlighted that the hybrid α-$Co(OH)_2$@Ni could be an encouraging transitional metal electrode material employed as an electrocatalyst for both the hydrogen and oxygen evolution reactions.

ASSOCIATED CONTENT

Determined double-layer capacitance, Electrochemical impedance spectroscopy, SEM pictures of Co-Ni-30 after stability test are in Supporting Information.

AUTHOR INFORMATION

Corresponding Author

Shan Ji (*): jishan@mail.zjxu.edu.cn, Tel./fax: +86 (0)15024355548

Hui Wang (**): wangh@qust.edu.cn, Tel./fax: +86(0)17866858722

Rongfang Wang (***): rfwang@qust.edu.cn, Tel./fax: +86(0)17686458002

Author Contributions

The manuscript was written through contributions of all authors. All authors have given approval to the final version of the manuscript.

Notes

The authors declare no competing financial interest.

ACKNOWLEDGMENT

The authors would like to thank the National Natural Science Foundation of China (21766032and 51661008).

REFERENCES

(1) Barbir, F. Transition to Renewable Energy Systems with Hydrogen as an Energy Carrier. *Energy* **2009,** *34*, 308-312.
(2) Ekinci, A.; Şahin, Ö.; Saka, C.; Avci, T. The Effects of Plasma Treatment on Electrochemical Activity of Co-W-B Catalyst for Hydrogen Production by Hydrolysis of $NaBH_4$. *Int. J. Hydrogen Energy* **2013,** *38* , 15295-15301.
(3) Lee, J. K.; Ann, H. H.; Yi, Y.; Lee, K. W.; Uhm, S.; Lee, J. A Stable Ni-B Catalyst in Hydrogen Generation via $NaBH_4$ Hydrolysis. *Catal. Commun.* **2011,** *16* , 120-123.
(4) Yan, Y.; Xia, B.; Zhao, B.; Wang, X. A Review on Noble-metal-free Bifunctional Heterogeneous Catalysts for Overall Electrochemical Water Splitting. *J. Mater. Chem. A* **2016,** *4* , 17587-17603.
(5) Ding, J.; Ji, S.; Wang, H.; Gai, H.; Liu, F.; Linkov, V.; Wang, R. Mesoporous Nickel-sulfide/nickel/N-doped Carbon as HER and OER Bifunctional Electrocatalyst for Water Electrolysis. *Int. J. Hydrogen Energy* **2019**, 44, 2832-2840.
(6) Ding, J.; Ji, S.; Wang, H.; Linkov, V.; Gai, H.; Liu, F.; Liu, Q.; Wang, R. N-Doped 3D Porous Ni/C Bifunctional Electrocatalysts for Alkaline Water Electrolysis. *ACS Sustain. Chem. Eng.* **2019,** *7* , 3974-3981.
(7) Ding, J.; Ji, S.; Wang, H.; Pollet, B. G.; Wang, R. Mesoporous CoS/ N-doped Carbon as HER and ORR Bifunctional Electrocatalyst for Water Electrolysers and Zinc-Air Batteries. *ChemCatChem* **2019**, 1026-1032.
(8) Li, X.; Niu, Z.; Jiang, J.; Ai, L. Cobalt Nanoparticles Embedded in Porous N-rich Carbon as an Efficient Bifunctional Electrocatalyst for Water Splitting. *J. Mater. Chem. A* **2016,** *4* , 3204-3209.
(9) Ding, J.; Wang, P.; Ji, S.; Wang, H.; Brett, D. J. L.; Wang, R. Mesoporous Nickel Selenide N-doped Carbon as a Robust Electrocatalyst for Overall Water Splitting. *Electrochim. Acta* **2019,** *300*, 93-101.
(10) Wang, Z.; Li, J.; Tian, X.; Wang, X.; Yu, Y.; Owusu, K. A.; He, L.; Mai, L. Porous Nickel-Iron Selenide Nanosheets as Highly Efficient Electrocatalysts for Oxygen Evolution Reaction. *ACS Appl. Mater. Interfaces* **2016,** *8* , 19386-92.
(11) Xu, Y.; Tu, W.; Zhang, B.; Yin, S.; Huang, Y.; Kraft, M.; Xu, R. Nickel Nanoparticles Encapsulated in Few-Layer Nitrogen-Doped Graphene Derived from Metal-Organic Frameworks as Efficient Bifunctional Electrocatalysts for Overall Water Splitting. *Adv. Mater.* **2017,** *29*, 1605957.
(12) Pan, L.; Zhang, H.; Li, L.; Yan, Z.; Ju, D.; Xu, C.; Ning, H.; Yu, W. Targeted Synthesis of Unique Nickel Sulfides (NiS, NiS_2) Micro-architectures and the Applications for the Enhanced Water Splitting System. *ACS Appl. Mater. Interfaces* **2017,** *9* , 2500-2508.
(13) Yang, Q.; Lv, C.; Huang, Z.; Zhang, C. Amorphous Film of Ternary NiCoP Alloy on Ni Foam for Efficient Hydrogen Evolution by Electroless Deposition. *Int. J. Hydrogen Energy* **2018,** *43* , 7872-7880.
(14) Kim, H.; Bae, S.; Jeon, D.; Ryu, J. Fully Solution-processable Cu_2O-$BiVO_4$ Photoelectrochemical Cells for Bias-free Solar Water Splitting. *Green Chem.* **2018,** *20* , 3732-3742.
(15) Li, R.; Zhou, D.; Luo, J.; Xu, W.; Li, J.; Li, S.; Cheng, P.; Yuan, D. The Urchin-like Sphere Arrays Co_3O_4 as a Bifunctional Catalyst for Hydrogen Evolution Reaction and Oxygen Evolution Reaction. *J. Power Sources* **2017,** 250-256.
(16) Ma, Y.; Wang, R.; Wang, H.; Key, J.; Ji, S. Control of MnO_2 Nanocrystal Shape From Tremella to Nanobelt for Ehancement of the Oxygen Reduction Reaction Activity. *J. Power Sources* **2015,** *280*, 526-532.
(17) Du, X.; Yang, Z.; Li, Y.; Gong, Y.; Zhao, M. Controlled Synthesis of $Ni(OH)_2$/Ni_3S_2 Hybrid Nanosheet Arrays as Highly Active and Stable Electrocatalysts for Water Splitting. *J. Mater. Chem. A* **2018,** *6* , 6938-6946.
(18) Friebel, D.; Louie, M. W.; Bajdich, M.; Sanwald, K. E.; Cai, Y.; Wise, A. M.; Cheng, M. J.; Sokaras, D.; Weng, T. C.; Alonso-Mori, R.; Davis, R. C.; Bargar, J. R.; Norskov, J. K.; Nilsson, A.; Bell, A. T. Identification of Highly Active Fe Sites in (Ni,Fe)OOH for Electrocatalytic Water Splitting. *J. Am. Chem. Soc.* **2015,** *137* , 1305-1313.
(19) Esswein, A. J.; Mcmurdo, M. J.; Ross, P. N.; Bell, A. T.; Tilley, T. D. Size-Dependent Activity of Co_3O_4 Nanoparticle Anodes for Alkaline Water Electrolysis. *J. Phys. Chem. C* **2009,** *113* , 15068-15072.
(20) Wang, J.; Zhang, W.; Zheng, Z.; Liu, J.; Yu, C.; Chen, Y.; Ma, K. Dendritic Core-shell Ni@Ni(Fe)OOH Metal/metal Oxyhydroxide Electrode for Efficient Oxygen Evolution Reaction. *Appl. Surf. Sci.* **2019,** *469*, 731-738.
(21) Wang, R.; Song, H.; Li, H.; Wang, H.; Mao, X.; Ji, S. Mesoporous Nitrogen-doped Carbon Derived From Carp with High Electrocatalytic Performance for Oxygen Reduction Reaction. *J. Power Sources* **2015,** *278*, 213-217.
(22) Wang, J.; Zhong, H. X.; Wang, Z. L.; Meng, F. L.; Zhang, X. B. Integrated Three-Dimensional Carbon Paper/Carbon Tubes/Cobalt-Sulfide Sheets as an Efficient Electrode for Overall Water Splitting. *ACS Nano* **2016,** *10* ,2342-2348.
(23) Zhang, Y.; Liu, Y.; Ma, M.; Ren, X.; Liu, Z.; Du, G.; Asiri, A. M.; Sun, X. A Mn-doped Ni_2P Nanosheet Array: an Efficient and Durable Hydrogen Evolution Reaction Electrocatalyst in Alkaline Media. *Chem. Commun.* **2017,** *53* ,

11048-11051.
(24) Yin, Z.; Zhu, C.; Li, C.; Zhang, S.; Zhang, X.; Chen, Y. Hierarchical Nickel-cobalt Phosphide Yolk-shell Spheres as Highly Active and Stable Bifunctional Electrocatalysts for Overall Water Splitting. *Nanoscale* **2016,** *8* , 19129-19138.
(25) Yang, Y.; Zhang, W.; Xiao, Y.; Shi, Z.; Cao, X.; Tang, Y.; Gao, Q. $CoNiSe_2$ Heteronanorods Decorated with Layered-double-hydroxides for Efficient Hydrogen Evolution. *Appl. Catal. B: Environ.* **2019,** *242*, 132-139.
(26) You, B.; Jiang, N.; Sheng, M.; Bhushan, M. W.; Sun, Y. Hierarchically Porous Urchin-Like Ni_2P Superstructures Supported on Nickel Foam as Efficient Bifunctional Electrocatalysts for Overall Water Splitting. *ACS Catal.* **2016,** *6* ,714-721.
(27) Cai, X.; Peng, M.; Yu, X.; Fu, Y.; Zou, D. Flexible Planar/fiber-architectured Supercapacitors for Wearable Energy Storage. *J. Mater. Chem. C* **2014,** *2* , 1184-1200.
(28) Zhu, J.; Tang, S.; Wu, J.; Shi, X.; Zhu, B.; Meng, X. Wearable High-Performance Supercapacitors Based on Silver-Sputtered Textiles with $FeCo_2S_4$-$NiCo_2S_4$ Composite Nanotube-Built Multitripod Architectures as Advanced Flexible Electrodes. *Adv. Energy Mater.* **2017,** *7* , 1601234.
(29) Wang, H.; Ren, Q.; Brett, D. J. L.; He, G.; Wang, R.; Key, J.; Ji, S. Double-shelled Tremella-like $NiO@Co_3O_4@MnO_2$ as a High-performance Cathode Material for Alkaline Supercapacitors. *J. Power Sources* **2017,** *343*, 76-82.
(30) Ren, Q.; Wang, R.; Wang, H.; Key, J.; Brett, D. J. L.; Ji, S.; Yin, S.; Kang Shen, P. Ranunculus Flower-like $Ni(OH)_2@Mn_2O_3$ as a High Specific Capacitance Cathode Material for Alkaline Supercapacitors. *J. Mater. Chem. A* **2016,** *4* , 7591-7595.
(31) Hu, Y.-M.; Liu, M.-C.; Hu, Y.-X.; Yang, Q.-Q.; Kong, L.-B.; Han, W.; Li, J.-J.; Kang, L. Design and Synthesis of $Ni_2P/Co_3V_2O_8$ Nanocomposite with Enhanced Electrochemical Capacitive Properties. *Electrochim. Acta* **2016,** *190*, 1041-1049.
(32) Niu, H.; Wang, Y.; Zhang, X.; Meng, Z.; Cai, Y. Easy Synthesis of Surface-Tunable Carbon-Encapsulated Magnetic Nanoparticles: Adsorbents for Selective Isolation and Preconcentration of Organic Pollutants. *ACS Appl. Mater. Interfaces* **2012,** *4* , 286-295.
(33) He, G.; Qiao, M.; Li, W.; Lu, Y.; Zhao, T.; Zou, R.; Li, B.; Darr, J. A.; Hu, J.; Titirici, M. M. S, N-Co-Doped Graphene-Nickel Cobalt Sulfide Aerogel: Improved Energy Storage and Electrocatalytic Performance. *Adv. Sci.* **2017,** *4* ,1600214.
(34) Liu, Q.; Wu, Z.; Ma, Z.; Dou, S.; Wu, J.; Tao, L.; Wang, X.; Ouyang, C.; Shen, A.; Wang, S. One-pot Synthesis of Nitrogen and Sulfur Co-doped Graphene Supported MoS_2 as High Performance Anode Materials for Llithium-ion Batteries. *Electrochim. Acta* **2015,** *177*, 298-303.
(35) Yang, L.; Liu, D.; Hao, S.; Kong, R.; Asiri, A. M.; Zhang, C.; Sun, X. A Cobalt-borate Nanosheet Array: an Efficient and Durable Non-noble-metal Electrocatalyst for Water Oxidation at Near Neutral pH. *J. Mater. Chem. A* **2017,** *5* , 7305-7308.
(36) Li, M.; Liu, X.; Xiong, Y.; Bo, X.; Zhang, Y.; Han, C.; Guo, L. Facile Synthesis of Various Highly Dispersive CoP Nanocrystal Embedded Carbon Matrices as Efficient Electrocatalysts for the Hydrogen Evolution Reaction. *J. Mater. Chem. A* **2015,** *3* , 4255-4265.

Graphical abstract